

Subtracting non-critical fluctuations in higher cumulants of conserved charges

Fan Zhang,¹ Zhiming Li,¹ Lizhu Chen,² Xue Pan,³ Mingmei Xu,¹ Yeyin Zhao,¹ Yu Zhou,⁴ and Yuanfang Wu¹

¹*Key Laboratory of Quark and Lepton Physics (MOE) and Institute of Particle Physics,
Central China Normal University, Wuhan 430079, China*

²*School of Physics and Optoelectronic Engineering,
Nanjing University of Information Science and Technology, Nanjing 210044, China*

³*School of Electronic Engineering, Chengdu Technological University, Chengdu 611730, China*

⁴*Department of Physics and Astronomy University of California Los Angeles, CA 90095, USA*

Using the sample produced by the AMPT default model, we construct a corresponding mixed sample by the method of mixed events. The mixed sample provides an effective estimation for non-critical fluctuations which are caused by global and systematic effects. The dynamical cumulants of conserved charges are defined as the cumulants of the original sample minus the cumulants of the mixed sample. It is demonstrated that dynamical cumulants are subtracted statistical fluctuations, and centrality bin width or detection efficiency independent, in consistent with formulae corrected cumulants. Therefore, dynamical cumulants are helpful in obtaining critical fluctuations at the RHIC BES.

PACS numbers: 25.75.Nq, 25.75.Gz

I. INTRODUCTION

To map QCD phase diagram from the experimental side, programs of beam energy scan (BES) I and II at relativistic heavy-ion collisions (RHIC) are suggested and in progress [1–5]. Higher cumulants of conserved charges are sensitive observable of critical fluctuations of quantum chromodynamics (QCD) phase transitions [6–18]. Their non-monotonic dependence of incident energy has been observed at the RHIC BES I [19, 20], and has drawn much of our attention [1, 4, 5].

It is clear there are non-critical fluctuations in measured cumulants, and numerous efforts have been made to eliminate non-critical effects [21–26]. A great challenge is how to properly subtract the non-critical fluctuations. It is crucial for determining the critical point (CP) of QCD phase transition at the current RHIC BES II program [5].

As we have known, critical fluctuations come from the inner correlations between particles of an event, where the correlation length is divergent.

Non-critical fluctuations have two kinds of sources. One is caused by conventional mechanisms, such as the resonance decay, and the global conservation of energy, momentum, and various charges. The length of these conventional correlations is finite and fixed. Their fluctuations are usually small in comparison to critical fluctuations, and result in a constant shift in cumulants [26].

Another source of non-critical fluctuations is global and systematic effects, such as the statistical fluctuations due to insufficient number of particles [23, 24], initial size fluctuations for different impact parameters [26–28], centrality bin width [22], detection efficiency and acceptance cuts [25].

In order to deduct one of those global and systematic effects, usually a specified scheme of correction is suggested. For example, statistical fluctuations are usually estimated by corresponding Poisson distribu-

tion [23, 29, 30]. Influence of centrality bin width is due to a given bin width composites a superposition of various impact parameters. Cumulants vary with bin width. To reduce the influence, a well known scheme, centrality bin width correction (CBWC), is proposed [31].

The detection efficiency in heavy ion experiment is the percentage of missing particles. It also affects the true distribution of particle number and its cumulants [25, 32]. To eliminate the influence, a complex formula which connect the true cumulant to the actually measured cumulant is introduced.

For a real world sample, all those global and systematic effects are involved. It is difficult to eliminate one of them. A good subtraction should take all of them into account. The *sample of mixed events* just provides a background of such [33].

The best mixed sample is shown to be constructed by the most random pool method [34]. There is no concerning correlations in measured cumulants of conserved charges. Meanwhile, non-critical fluctuations due to global and systematic effects retain. This mixed sample provides a possible estimation for the cumulants of back-ground. We can define dynamical cumulants as the cumulants of the original sample minus the cumulants of the mixed sample. Such defined dynamical cumulants subtract non-critical fluctuations remaining in the mixed sample, and extract critical fluctuations.

In this paper, we first introduce the construction of mixed sample for higher cumulants of conserved charges in Section II. Then, In section III, using the sample of Au + Au collisions at 19.6 GeV produced by a multi-phase transport (AMPT) default model, we construct its mixed sample at each centrality bin. Higher cumulants of net-proton in the original and mixed samples are calculated and compared. The influences of statistical fluctuations, centrality bin width, and efficiency are studied respectively. The dynamical cumulants are shown to be independent of centrality bin width or efficiency, in con-

sistent with formula corrected cumulants. Finally, a brief summary and conclusions are given in section IV.

II. MIXED SAMPLE

Higher cumulants of conserved charges are defined as variance (σ^2), skewness (S), kurtosis (κ), and their products, $S\sigma$ and $\kappa\sigma^2$, i.e.,

$$\begin{aligned}\sigma^2 &= \langle (\Delta N_c)^2 \rangle, \\ S &= \langle (\Delta N_c)^3 \rangle / \sigma^3, \\ \kappa &= \langle (\Delta N_c)^4 \rangle / \sigma^4 - 3, \\ S\sigma &= \langle (\Delta N_c)^3 \rangle / \sigma^2, \\ \kappa\sigma^2 &= \langle (\Delta N_c)^4 \rangle / \sigma^2 - 3\sigma^2.\end{aligned}\quad (1)$$

Where the average $\langle \rangle$ is over the whole event sample. $\Delta N_c = N_c - \langle N_c \rangle$. N_c is the number of particles with conserved charges. In general, conserved charge refers to baryon, strangeness, or electric charge. In this paper, we restrict the conserved charge to baryon, or strangeness only. The total number of particles of an event is electric charged, i.e, N_{ch} , multiplicity.

By definition, Eq. ((1)), N_c is correlated with its associated event. N_c charged particles correlate with each other and with other $N_{\text{ch}} - N_c$ particles. For a mixed event, all such correlations have to be removed. Meanwhile, the global characters of the mixed sample, such as, the multiplicity N_{ch} distribution, and the mean number of charged particles $\langle N_c \rangle$ should retain. They directly relate to initial size fluctuations, statistical fluctuations, detection efficiency, and acceptance cuts.

We have shown that the pool method [34] is effective in constructing mixed sample for higher cumulants of conserved charges. Where the multiplicity N_{ch} is simply taken from the original sample. All particles of original events is firstly put into a pool, and then randomly take N_{ch} particles from the pool to form a mixed event. When the sample is large enough, i.e., larger than a thousand events, N_{ch} particles come approximately from different events and the correlations between them are negligible. Meanwhile, it has shown that the mean number of charged particles $\langle N_c \rangle$ is consistent with that of the original sample.

For a given sample, the mixed sample can be constructed by this pool method. For convenience in following statements, we label cumulants of the original and mixed samples by superscripts o and m , respectively. We define the dynamical cumulant as the cumulant of the original sample minus the cumulant of the mixed sample, i.e.,

$$\begin{aligned}\sigma_{\text{dyn}}^2 &= \sigma^{2,o} - \sigma^{2,m}, \\ S_{\text{dyn}} &= S^o - S^m, \\ \kappa_{\text{dyn}} &= \kappa^o - \kappa^m, \\ S\sigma_{\text{dyn}} &= (S\sigma)^o - (S\sigma)^m, \\ \kappa\sigma_{\text{dyn}}^2 &= (\kappa\sigma^2)^o - (\kappa\sigma^2)^m.\end{aligned}\quad (2)$$

Obviously, global and systematic effects in the mixed sample are subtracted by defined dynamical cumulants. In order to demonstrate the effectiveness of dynamical cumulants, we will firstly apply the pool method to construct a mixed sample in the following, and then compare dynamical cumulants with formulae corrected cumulants, which are labelled as σ_{fc}^2 , S_{fc} , κ_{fc} , $S\sigma_{\text{fc}}$, and $\kappa\sigma_{\text{fc}}^2$, respectively.

III. APPLICATION AND COMPARISON

We generate a sample of Au + Au collisions at 19.6 GeV by the AMPT default model. Where the multiplicity is total electric charged particles, i.e., N_{ch} , and the net-proton is considered approximately as net-baryon [35–37], i.e., $N_c = N_p$. Cuts for transverse momentum and rapidity are $0.4 \leq p_t \leq 0.8$ (GeV) and $-0.5 \leq y \leq 0.5$, the same as those used at the RHIC/STAR experiments [38].

As described in the Introduction Section, up to now, only statistical fluctuations [23, 24, 29], the influence of centrality bin width and detection efficiency are corrected respectively by corresponding formulae [25, 39]. In the following, we will compare dynamical cumulants with corresponding formula corrected cumulants, respectively.

A. Statistical fluctuations

The centrality dependences of $S\sigma$ and $\kappa\sigma^2$ of original (black circles) and mixed (red open squares) samples are presented in Fig. 1(a) and (c). Where 9 centralities are divided as those given at the RHIC/STAR [38]. The centrality dependence of dynamical (violet open crosses) and formula corrected (blue open diamonds) $S\sigma$ and $\kappa\sigma^2$ are presented in Fig. 1(b) and (d). Where, the statistical fluctuations are described by a Poisson distribution with $\langle N_c \rangle$ of the original sample [23, 24, 29]. Formula corrected cumulants are the original cumulants minus the cumulants of corresponding Poisson distribution.

Fig. 1(a) shows that $S\sigma$ of the mixed sample, i.e., $S\sigma^m$, red open squares, have generally similar centrality dependence as those of the original sample, i.e., $S\sigma^o$, black circles. Red open squares are close to those of black circles, except one for the most central collision.

In Fig. 1(b), most of $S\sigma_{\text{dyn}}$, violet open crosses, are flat and show a low shift to those of $S\sigma_{\text{fc}}$, blue open diamonds. Only for the most central collision, the violet open crosses almost overlaps with the blue open diamonds.

Differences between $S\sigma_{\text{dyn}}$ and $S\sigma_{\text{fc}}$ are understandable. As we have discussed in the Introduction Section, the mixed sample contains all global and systematic effects, dynamical cumulants deduct all of them in the mixed sample. Here, formula corrected cumulant only deducted Poisson-like statistical fluctuations. Other global effects, in particular, the initial size fluctuations remain

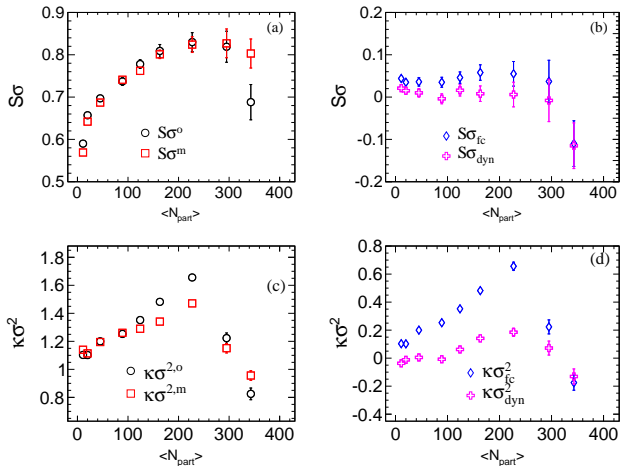


FIG. 1. Left: the centrality dependence of $S\sigma$ (a) and $\kappa\sigma^2$ (c) for the original and mixed samples. Right: the centrality dependence of dynamical and formula corrected $S\sigma$ (b) and $\kappa\sigma^2$ (d).

in the formula corrected cumulants. So the formula corrected cumulants are larger than those of dynamical cumulants.

Fig. 1(c) also shows that the general trend of the centrality dependence of $\kappa\sigma^2$ of the mixed sample is analogous with that of the original sample. The differences between them are visible, or larger, in comparison to the corresponding cases of $S\sigma$ in Fig. 1(a). In Fig. 1(d), the centrality dependence of $\kappa\sigma_{\text{dyn}}^2$ is qualitatively similar to that of $\kappa\sigma_{\text{fc}}^2$, but much smooth and lower than that of $\kappa\sigma_{\text{fc}}^2$.

So in general, dynamical cumulants are smaller than formula corrected cumulants, where only Poisson-like statistical fluctuations are subtracted. This implies that mixed sample contains other non-critical effects in addition to Poisson-like statistical fluctuations. We will show in the following that dynamical cumulants also eliminate influences of centrality bin width and detection efficiency.

It should be noticed although dynamical cumulants showed in Fig. 1(b) and (d) are very small, but not zero. As we known, there is no phase transition in the AMPT default model. So there should be no critical fluctuations. However, conventional mechanisms are implemented in the model. Those conventional correlations exist in the original sample but do not retain in the mixed sample. Therefore, dynamical cumulants just present those conventional correlations, which are not zero.

B. Centrality bin width

In Fig. 2(a), we present centrality dependence of $\kappa\sigma^2$ of the original sample for nine (black solid points) and sixteen (red circles) centrality bins. Red circles are obvi-

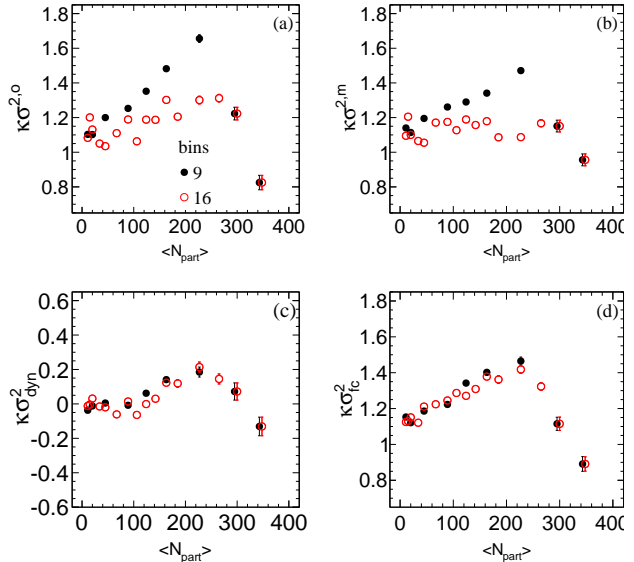


FIG. 2. The centrality dependence of $\kappa\sigma^2$ of original (a) and mixed (b) samples for nine (black points) and sixteen (red circles) centrality bins, and the centrality dependence of dynamical (c) and formula corrected (d) $\kappa\sigma^2$ for nine (black points) and sixteen (red circles) centrality bins.

ously smaller than those black solid points. So $\kappa\sigma^2$ varies with centrality bin width.

Using the corrected formulae Eq. (5) and Eq. (12) of ref. [22] and Eq. (28) of ref. [40], the corrected $\kappa\sigma^2$ for nine (black points) and sixteen (red circles) centrality bins are presented in Fig. 2(d). Where red and black points are close to each other. So $\kappa\sigma_{\text{fc}}^2$ are centrality bin width independent. Therefore, formula corrected cumulants successfully eliminate the influence of centrality bin width.

At each of centrality bin, we construct mixed sample. The corresponding centrality dependences of $\kappa\sigma^2$ for nine (black solid points) and sixteen (red circles) centrality bins are presented in Fig. 2(b). The influence of centrality bin width is similar to the case of the original sample as showed in Fig. 2(a).

Centrality dependences of dynamical cumulants ($\kappa\sigma_{\text{dyn}}^2$) for nine (black points) and sixteen (red circles) centrality bins are presented in Fig. 2(c). The black solid points and red circles are close to each other. This shows that dynamical cumulants are centrality bin width independent, similar to formula corrected cumulants in Fig. 2(d). This is understandable. Since the mixed sample contains similar influences of centrality bin width as those of the original sample, the dynamical cumulants are well deducted the influence of centrality bin width remaining in the mixed sample.

It should be noticed that the magnitude of dynamical cumulants in Fig. 2(c) is smaller than that of formula corrected cumulants in Fig. 2(d). The dynamical cumulants

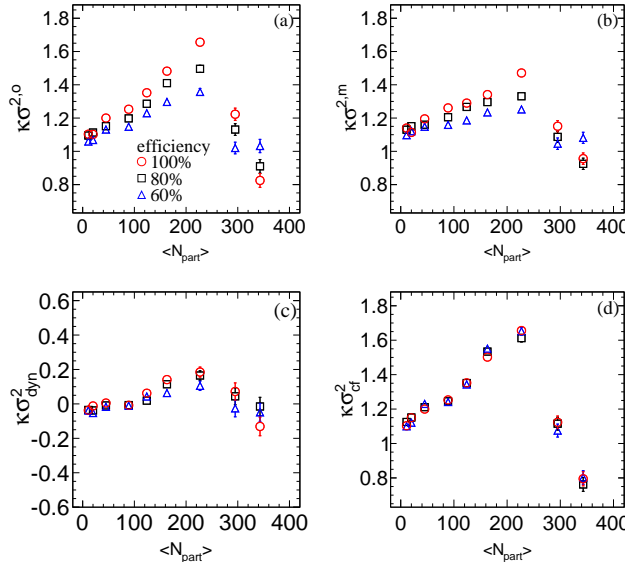


FIG. 3. The centrality dependences of $\kappa\sigma^2$ of original (a) and mixed (b) samples for three efficiencies, 100% (red circles), 80% (black squares), and 60% (blue triangles), and the centrality dependence of dynamical (c) and formula corrected (d) $\kappa\sigma^2$ for three efficiencies, 100% (black points), 80% (black squares), and 60% (blue triangles).

in Fig. 2(c) are the same magnitude as those dynamical cumulants in Fig 1(d), where the statistical fluctuations are also subtracted. dynamical cumulants eliminate not only the statistical fluctuations, but also the influence of centrality bin width. However, formula corrected cumulants in Fig. 2(d) are not subtracted the statistical fluctuations. This is why dynamical cumulants are smaller than that of formula corrected cumulants.

For other cumulants of net-proton, plots like those showed in Fig. 2 are not presented. Their dynamical cumulants also show centrality bin width independence as that of $\kappa\sigma_{\text{dyn}}^2$ do.

C. Detection efficiency

To see the influence of detection efficiency, we can randomly take 80% and 60% of produced particles, and calculate corresponding cumulants. The centrality dependency of $\kappa\sigma^2$ of original sample for three efficiencies, 100% (black points), 80% (black squares), and 60% (blue triangles) are presented in Fig. 3(a). It shows that three kinds of points are separated. Cumulants vary with efficiency. The influence of efficiency is centrality dependent.

The centrality dependences of $\kappa\sigma^2$ of mixed sample for three efficiencies, 100% (red circles), 80% (black squares), and 60% (blue triangles) are presented in Fig. 3(b). Efficiency also influence measured cumulants of mixed sample. The influences are similar to that of the original

sample showed in Fig. 3(a).

Using the formula Eq. (26) of ref. [25] and Eqs. (A20), (A23), (A25), and (A28) of ref. [39], the centrality dependency of formula corrected $\kappa\sigma^2$ for three efficiencies, 100% (red circles), 80% (black squares), and 60% (blue triangles) are presented in Fig. 3(d). Where black squares and blue triangles overlap with those red circles within errors at each of centralities. This means $\kappa\sigma_{\text{fc}}^2$ is efficiency independent.

The centrality dependency of dynamical $\kappa\sigma^2$ for three efficiencies, 100% (black points), 80% (black squares), and 60% (blue triangles) are presented in Fig. 3(c). Where three kinds of points overlap within errors. It shows dynamical $\kappa\sigma^2$ is also efficiency independent. This is because the mixed sample contains the same influence of efficiency as that of the original sample. dynamical cumulants subtract the influence of efficiency remaining in the mixed sample.

The values of those points in Fig. 3(c) are the same magnitude as dynamical cumulants in Fig 1(d), where the statistical fluctuations are subtracted. So dynamical cumulants subtract not only the influence of detection efficiency, but also the statistical fluctuations, and the influence of centrality bin width. While, formula corrected cumulants in Fig. 3(d) subtract only the influence of efficiency.

For other cumulants of net-proton, plots like those showed in Fig. 3 are not presented. Their dynamical cumulants also show efficiency independence as $\kappa\sigma_{\text{dyn}}^2$ do.

IV. SUMMARY AND CONCLUSIONS

In the paper, we generate the original sample of Au + Au collisions at 19.6 GeV by the AMPT default model, and construct its mixed sample at each centrality bin. The mixed sample retain the original multiplicity distribution. Electric charged particles of a mixed event are randomly taken from the pool of all particles of the original events at a given centrality. So the mixed sample retains the global and systematic characters of the original sample and loses all concerning correlations in cumulants of conserved charges.

The centrality dependence of net-proton cumulants for the original and mixed samples are presented and compared. We define dynamical cumulants as the cumulants of the original sample minus the cumulants of the mixed sample. It shows that dynamical cumulants is subtracted statistical fluctuations. Moreover, dynamical cumulants are both centrality bin width independent and detection efficiency independent. These are consistent with the cumulants which are corrected by formulae of centrality bin width correction (CBWC), or detection efficiency. Therefore, dynamical cumulants are free from influences of centrality bin width and detection efficiency.

In conclusion, the mixed sample provides a good estimation for global and systematic non-critical effects. The defined dynamical cumulants substantially subtract

influences of non-critical effects contained in the mixed sample. It helps us to obtain true critical fluctuations from higher cumulants of conserved charges at the RHIC BES.

V. ACKNOWLEDGEMENT

This work is supported in part by the Ministry of Science and Technology (MoST) under grant No. 2016YFE0104800.

-
- [1] S. Gupta, X. Luo, and B et al. Mohanty. *Science*, 332:1525–1528, (2011).
- [2] M.M.Aggarwal et al.(STAR Collaboration). *arXiv*, 1007:2613, (2010).
- [3] X. Luo. *Nucl.Phys.A*, 956:75–82, (2016).
- [4] X. Luo. *Nucl.Phys.A*, 904-905:911c–914c, 2013.
- [5] STAR Note 0598. BES-II whitepaper.
- [6] M. Stephanov, K. Rajagopal, and E. Shuryak. *Phys.Rev.Lett*, 81:4816, (1998).
- [7] M. Stephanov, K. Rajagopal, and E. Shuryak. *Phys.Rev.D*, 60:114028, (1999).
- [8] S. Jeon and V. Koch. *Phys.Rev.Lett*, 83:5435, (1999).
- [9] M. Asakawa, U. Heinz, and B. Muller. *Phys.Rev.Lett*, 85:2072, (2000).
- [10] V. Koch, A. Majumder, and J. Randrup. *Phys.Rev.Lett*, 95:182301, (2005).
- [11] S. Ejiri, F. Karsch, and K. Redlich. *Phys.Lett.B*, 633:275–282, (2006).
- [12] C. Athanasiou, K. Rajagopal, and M. Stephanov. *Phys.Rev.D*, 82:074008, (2010).
- [13] M.A. Stephanov. 102:032301, (2009).
- [14] M.A. Stephanov. *Phys.Rev.Lett*, 107:052301, (2011).
- [15] Y. Hatta and M.A. Stephanov. *Phys.Rev.Lett*, 91:102003, (2003).
- [16] M. Cheng, P. Hegde, and C. et al. Jung. *Eur.Phys.J.C*, 71:1694, (2011).
- [17] K. Morita, B. Friman, and K. Redlich. *Phys.Lett.B*, 741:178–183, (2015).
- [18] M. Asakawa, S. Ejiri, and M. Kitazawa. *Phys.Rev.Lett*, 103:262301, (2009).
- [19] L. Adamczyk et al.(STAR Collaboration). *Phys.Rev.Lett*, 113:092301, (2014).
- [20] L. Adamczyk et al.(STAR Collaboration). *Phys.Rev.Lett*, 112:032302, (2014).
- [21] A. Bzdak, V. Koch, and V. Skokov. *Phys.Rev.C*, 87:014901, 2013.
- [22] X. Luo. *J.Phys.C.S*, 316:012003, (2011).
- [23] Xue Pan, Fan Zhang, Zhiming Li, Lizhu Chen, Mingmei Xu, and Yuanfang Wu. *Phys.Rev.C*, 89:014904, (2014).
- [24] Dai-Mei Zhou, Ayut Limphirat, Yu-liang Yan, Cheng Yun, Yu-peng Yan, Xu Cai, Laszlo p. Csernai, and Ben-Hao Sa. *Phys.Rev.C*, 85:064916, (2012).
- [25] A. Bzdak and V. Koch. *Phys.Rev.C*, 91:027901, (2015).
- [26] Lijia Jiang, Pengfei Li, and Huichao Song. *Phys.Rev.C*, 94:024918, (2016).
- [27] Jixing Li, Hao-jie Xu, and Huichao Song. *Phys.Rev.C*, 97:014902, 2018.
- [28] Lijia Jiang, Pengfei Li, and Huichao Song. *N.Phys.A*, 956:360–364, 2016.
- [29] Lizhu Chen, Xue Pan, Fengbo Xiong, Lin Li, Na Li, Zhiming Li, Gang Wang, and Yuanfang Wu. *J.Phys.G:Nucl.Part.Phys*, 38:11504, (2011).
- [30] Lizhu Chen, Zhiming Li, Xia Zhong, Yuncun He, and Yuanfang Wu. *J.Phys.G:Nucl.Part.Phys*, 42:065103, (2015).
- [31] X. Luo. *arXiv:1503.02558*, (2015).
- [32] A. Bzdak and V. Koch. *Phys.Rev.C*, 91:027901, (2015).
- [33] M.Gazdzicki, M.I.Gorenstein, and M.M.Pawlowska. *Phys.Rev.C*, 88:024907, (2013).
- [34] F Zhang, Zhiming Li, Lizhu Chen, Xue Pan, Xu.Mingmei, ZhaoYeyin, Yu Zhou, and Yuanfang Wu. *arXiv*, 1908.05465, (2019).
- [35] Y.Hatta and M.A.Stephanov. *Phys.Rev.Lett*, 91:102003, (2003).
- [36] M.M.Aggarwal et al.(STAR Collaboration). *Phys.Rev.Lett*, 105:022302, (2010).
- [37] P.Costa, M.C.Ruivo, and C.A.de Sousa. *Phys.Rev.D*, 77:096001, (2008).
- [38] M.M.Aggarwal et al.(STAR Collaboration). *Phys.Rev.Lett*, 105:022302, (2010).
- [39] X. Luo. *Phys.Rev.C*, 91:034907, (2015).
- [40] X. Luo. *J.Phys.G:Nucl.Part.Phys*, 39:025008, (2012).